

Article

Solar Heterogenous Photocatalytic Degradation of Methylthionine Chloride on a Flat Plate Reactor: Effect of pH and H₂O₂ Addition

Pablo E. Zaruma-Arias ¹, Cynthia M. Núñez-Núñez ² , Luis A. González-Burciaga ¹ and José B. Proal-Nájera ^{1,*} 

¹ Instituto Politécnico Nacional, CIIDIR-Unidad Durango, Calle Sigma 119, Fracc. 20 de Noviembre II, Durango 34220, Mexico; rycarpablo@hotmail.com (P.E.Z.-A.); luis.gonzalez.iq@gmail.com (L.A.G.-B.)

² Ingeniería en Tecnología Ambiental, Universidad Politécnica de Durango, Carretera Durango-México km 9.5, Col. Dolores Hidalgo, Durango 34300, Mexico; cynthia.nunez@unipolidgo.edu.mx

* Correspondence: jproal@ipn.mx

Abstract: Methylthionine chloride (MTC) is a compound with several applications both in the clinical and medical industries. Nevertheless, such compounds can become an environmental problem, as they are not properly treated by wastewater treatment plants. This objective of this work was to study MTC degradation in a flat plate reactor through solar photolysis and heterogeneous photocatalysis processes with TiO₂ as a catalyst. In addition to the processes, three pH (3.5, 6.5, and 9) and the effect of H₂O₂ addition (no dose, 0.5, and 1 mM/L) were tested. The results show that acidic pH is the most appropriate for MTC degradation, which ranged between 56% and 68.7% for photolysis and between 76% and 86.7% in photocatalysis. The H₂O₂ addition resulted in lower degradation in all cases, leading the authors to conclude that the presence of peroxide actually hinders degradation in solar photolysis and photocatalysis processes. Statistical analysis showed that the constant rate reactions calculated for every process, under the same conditions of pH and H₂O₂ addition, are significantly different from one another, and the three factors considered for experimental design (process, pH, and H₂O₂) have a statistically significant effect on MTC degradation. The collector area per order confirmed higher efficiency for photocatalysis when compared to photolysis processes.

Keywords: advanced oxidation processes; batch mode; solar radiation; solar-driven systems; titanium dioxide



Citation: Zaruma-Arias, P.E.; Núñez-Núñez, C.M.; González-Burciaga, L.A.; Proal-Nájera, J.B. Solar Heterogenous Photocatalytic Degradation of Methylthionine Chloride on a Flat Plate Reactor: Effect of pH and H₂O₂ Addition. *Catalysts* **2022**, *12*, 132. <https://doi.org/10.3390/catal12020132>

Academic Editor: Antonio Eduardo Palomares

Received: 22 December 2021

Accepted: 18 January 2022

Published: 21 January 2022

Publisher's Note: MDPI stays neutral with regard to jurisdictional claims in published maps and institutional affiliations.



Copyright: © 2022 by the authors. Licensee MDPI, Basel, Switzerland. This article is an open access article distributed under the terms and conditions of the Creative Commons Attribution (CC BY) license (<https://creativecommons.org/licenses/by/4.0/>).

1. Introduction

Methylthionine chloride (MTC) is a cationic heterocyclic aromatic chemical compound with a molecular formula of C₁₆H₁₈ClN₃S (Figure 1). MTC is a green shiny powder that is very soluble in water and confers a blue color to the solution [1–3], which is usually known as methylene blue and is signally used in different industrial sectors [4], such as textile [5], chemical, and clinical, since it is considered a safe and effective substance [6–8].

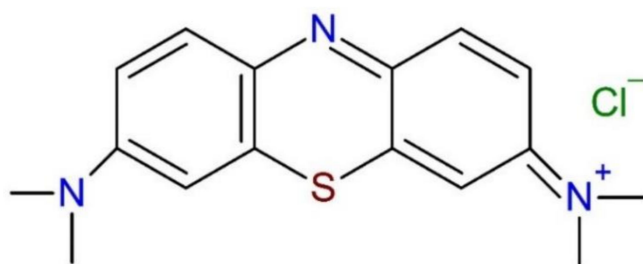


Figure 1. Methylthionine chloride molecule structure.

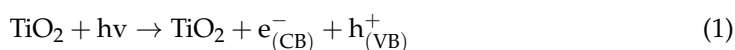
MTC has been widely used in the clinical field for photodynamic therapy and as an indicator of breast cancer [9–12], for the treatment of urinary tract infections [13,14], or even

malaria [15,16]. In textiles and painting industries, the MTC is used as a dye for painting different fabrics such as cotton, silk, wool, and leather [17,18]. MTC is also frequently used in aquaculture to cure diseases, disinfect, and transport fish [19,20]. At the laboratory level, MTC is used for the initial microscopic examination of macroscopically negative blood cultures [21].

MTC is a synthetic substance, with a chemical structure difficult to break, making it an extremely hard compound to remove by traditional mechanical or biological methods, principally due their N group [22]. Annually, the production of this type of compounds is about 700,000–10,000,000 t [23–25], and $\approx 280,000$ t of dyes are released into water bodies and end in traditional wastewater treatment plants [23,24] where they are considered urban wastes and treated with primary and secondary treatments but only reaching 20% and 60% of removal, respectively [26]. These substances can cause negative and counterproductive effects in water bodies, contaminating the ecosystem and the species that inhabit it [27]. This not only aesthetically affects an ecosystem but also causes a serious disturbance in photosynthetic activity due to the low penetration of solar radiation, progressing directly to living organisms [28–30]. As a result of this, is necessary to find a suitable method for the removal or degradation of substances.

The most appropriate treatments against recalcitrant compounds are advanced oxidation processes (AOPs) mainly by their generation of a powerful chemical agent, the hydroxyl radical ($\bullet\text{OH}$, 2.8 eV oxidative potential) [31–33]. Heterogeneous photocatalysis, one of the AOPs, normally uses TiO_2 as a catalyst and UV radiation; this generates gaps in electron pairs, which reach and break bonds of molecules [34].

Figure 2 shows the general mechanism of heterogeneous photocatalysis. The reaction in Equation (1) takes place when a beam of light containing photons with a wavelength less than or equal to 387 nm (UV-A region of the electromagnetic spectrum) falls on the surface of the photocatalyst, generating the electron–hole pair ($e^-_{(\text{CB})}$, $h^+_{(\text{VB})}$) due to the migration of electrons from the valence band (VB) to the conduction band (CB).



The main equations of the mechanism for reactive radical species generation by photocatalysis are shown in the Section (S1) in Supplementary Materials.

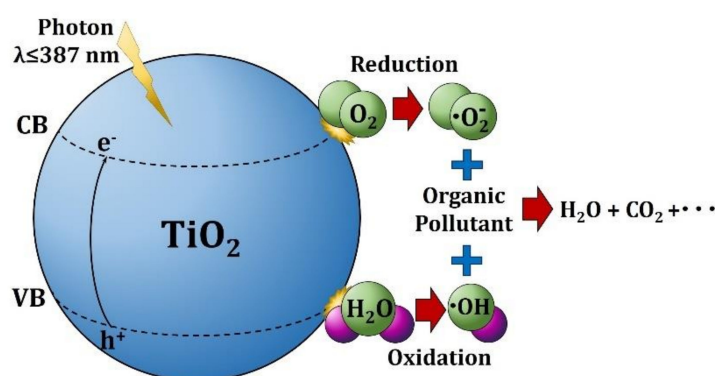


Figure 2. General mechanism of heterogenous photocatalysis.

The most active species responsible for carrying out the oxidation in the photocatalytic process are the $\bullet\text{OH}$, superoxide radical ($\bullet\text{O}_2^-$), and the hydroperoxide radical ($\bullet\text{HO}_2$). Radical $\bullet\text{OH}$ has a redox potential of 2.8 eV, being greater than other reactive species such as O_3 (2.1 eV), Cl (2.03 eV), H_2O_2 (1.8 eV), and CO_3^- (1.59 eV), among many others [35]. The OH redox potential is greater even than that generated by the holes (h^+) produced in the photocatalyst band jump (2.53 eV) [36,37]. These reactive species can degrade pollutants in a fast and non-selective manner until mineralization to produce non-toxic substances [38]. The great oxidizing power of $\bullet\text{OH}$ makes it capable of degrading most

organic and organometallic pollutants until their mineralization by transforming them into CO₂, water, and inorganic ions [39]. Photocatalysis has been used to degrade this type of recalcitrant substances, obtaining positive results [40].

There are different types of reactors for wastewater treatment by heterogeneous photocatalysis, but they all have an exclusively designated place in the system for fixing the semiconductor, which will receive UV radiation artificially, with a UV lamp, or natural solar radiation [41]. Flat plate photocatalytic reactors using natural solar radiation have been recognized as a suitable alternative, which is largely due to their low manufacturing and maintenance cost. The countries in the planet's Sunbelt are the most appropriate for using this type of technology with natural solar radiation, given that they receive an average annual solar irradiation of 5.5 kWh/m²/day, and on occasions, it can reach 6.5 kWh/m²/day [42].

Flat plate solar reactors used in heterogeneous photocatalysis have been receiving great interest as an alternative application due to their low cost of manufacture and maintenance [43]. However, the main challenge of these reactors lies in having enough solar radiation to penetrate and distribute itself over a large contact surface of the photocatalyst. Freudenhammer et al. [44] report results of a pilot study with fixed bed and thin film reactors (TFFBR) for the treatment of wastewater from the textile industry.

Non-concentrated flat plate reactors have significant advantages and simple structure, because they do not use mechanical parts or solar-tracking devices, they have a low production cost, and they are easier and cheaper to install compared to systems with concentration; however, their design must be carefully thought out with the requirements for chemical stability, weather resistance, and UV light in mind [45,46]. Since these reactors do not have a photon concentrator, diffuse light can be captured without the need for a reflective surface, which eliminates the loss of efficiency that other types of reactors present [47].

The aim of this work was to degrade the MTC compound by photolysis and heterogeneous photocatalysis in a flat plate reactor, with TiO₂ as a catalyst and solar radiation as the activation energy. In addition, the effects of different pH levels and doses of hydrogen peroxide (H₂O₂) on the degradation efficiency of MTC were evaluated by kinetic and statistical analysis, comparing the MTC degradation efficiency. Collector area per order (A_{CO})(m²/m³-order) was also estimated for the evaluation of AOPs in aspects of energy requirements or area required.

2. Results and Discussion

According to Dean et al. [42], in low MTC concentrations, the dimer formation does not take place. The initial concentration of MTC to perform the experiments was 30 mg/L, which was selected in order to avoid dimer formation, as such a formation could intervene with absorbance reading. As the absorbance reading at 670 nm was used to calculate the MTC concentration on samples, the method could have been affected for the absorbance of 605 nm, which is the maximum absorbance for MTC dimers [48].

According to Houas et al. [49], one hour is required to reach MTC and TiO₂ adsorption equilibrium; as experiments lasted for only 60 min, it was important to reject the possibility that only the adsorption of MTC molecules on the TiO₂ surface (on photocatalysis experiments) was to be blamed for the degradation results. Such a possibility was rejected by the results of control experiments.

Control experiments lasted for 60 min, similarly to regular experiments, but in the absence of radiation. The results were always lower than 10%, so only the absorbance of MTC on the photocatalyst or support was rejected as the explanation for the degradation.

It is known that in basic solutions, MTC can transform to trimethylthionine [48]; such a transformation was discarded by the MTC concentration reading in control experiments, which were performed in the absence of radiation. Trimethylthionine is a phenothiazine derivative dye that presents redox activity [50].

When H_2O_2 was added to control experiments, MTC degradation was not remarkable; these results allowed authors to discard oxidant presence as the main factor acting in the processes. The highest degradation by H_2O_2 addition in control photolysis experiments was 6% in a neutral pH.

2.1. MTC Degradation by Photolysis

The photolytic degradation of MTC ranged from 3.27% to 68.68% after 60 min of experimentation. Of the three pH magnitudes tested, acidic pH yielded the best results, which are portrayed in Figure 3. Actually, at the higher pH, the degradation was lower (Table 1).

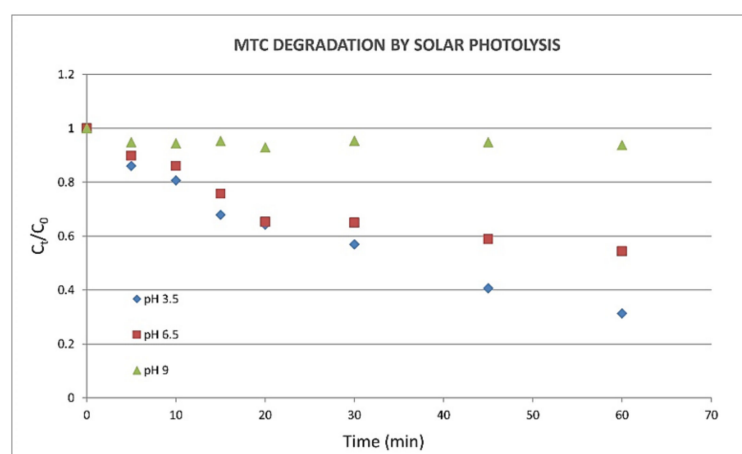


Figure 3. MTC degradation by solar photolysis at different pH (3.5, 6.5, and 9) without H_2O_2 addition.

Table 1. MTC degradation percentage and kinetic parameters calculated for photolytic and photocatalytic processes under three different pH (3.5, 6.5, and 9) and H_2O_2 doses (no dose, 0.5, and 1 mM/L).

pH	Photolysis					Photocatalysis			
	H_2O_2 (mM/L)	K_{ph} (min^{-1})	Error	$\tau_{1/2}$ (min)	Degradation (%)	K_{phC} (min^{-1})	Error	$\tau_{1/2}$ (min)	Degradation (%)
3.5	0	0.0199	0.000538	34.90	68.68	0.0340	0.000704	20.37	86.68
	0.5	0.0151	0.001216	45.76	56.14	0.0255	0.002014	27.18	75.22
	1	0.0143	0.000867	48.42	56.26	0.0276	0.002333	25.15	76.26
6.5	0	0.0121	0.001125	57.36	45.56	0.0222	0.003326	31.26	63.73
	0.5	0.0113	0.001537	61.24	41.22	0.0225	0.001575	30.80	69.44
	1	0.0103	0.001493	67.55	39.43	0.0153	0.001542	45.35	53.77
9	0	0.0015	0.000379	470.20	6.28	0.0181	0.002466	38.30	57.17
	0.5	0.0093	0.001157	74.16	36.53	0.0093	0.001146	74.18	38.43
	1	0.0012	0.000359	599.80	3.27	0.0043	0.000504	160.71	18.74

Figure 3 portrays the variation of concentration (mg/L) at each time for the degradation of MTC in aqueous solution when treated by photolysis in a solar photocatalytic reactor (SPR), without photocatalyst, at different pH and without H_2O_2 addition. As shown in Figure 3, degradation of 68.68% was achieved under acidic pH, being the highest degradation reached in this experimental series.

When photodegradation experiments take part using a UV-C lamp as the source of radiation, H_2O_2 addition improves results, given the formation of $\bullet\text{OH}$ radicals after peroxide breakup [51]; in this case, as experiments were performed using solar radiation, H_2O_2 addition actually hinders MTC degradation.

Given that H_2O_2 addition in control experiments does not show degradation, but in experiments in the presence of radiation, it actually hinders the degradation, the authors believe this to be an indication of competence for radiation between MTC and peroxide molecules.

Zhou et al. [52] degraded only 13% under pH 7, when solar radiation was applied to a MTC solution with a 400 mg/L concentration. For near-neutral pH, degradation in this study reached 45%; nevertheless, comparison is difficult, as the initial concentration here considered is lower (30 mg/L).

Djellabi et al. [53] reported in their study a low MTC degradation, reaching 9% after 5 h of experiments, in acid pH condition (2.7) and 10^{-2} M of H_2O_2 , but with solar sunlight radiation intensity below that reported in this study.

In near-neutral pH (6.5), a maximum degradation of 45% of MTC was obtained without oxidant agent addition, 41.22% with 0.5 mM, and 39.43% when 1 mM was added. These results are proximate to those reported by Benhabiles et al. [54], where their photolysis experiments reached 35% contaminant degradation, in similar pH conditions, without H_2O_2 addition, and solar irradiation above 650 W/m^2 .

Conversely, in basic pH condition, the best degradation percentage of MTC was obtained when 0.5 mM of H_2O_2 was added, reaching 36.53%, but without the addition and dose of 1 mM, presenting 6.28% and 3.27%, in that order.

2.2. Solar Heterogeneous Photocatalysis to Degrade MTC

Experiments performed in the presence of photocatalyst were always better than those of photolysis (Table 1). The highest degradation was reached in a photocatalysis experiment, without H_2O_2 addition and in acidic pH. In these experiments, as in photolysis (Section 2.1), H_2O_2 addition hinders degradation but only for acidic and basic pH. Under neutral pH, the addition of 0.5 mM/L of peroxide slightly improves degradation.

The results of degradation of MTC by solar heterogeneous photocatalysis without H_2O_2 addition on three different pH magnitudes are portrayed in Figure 4. As can be noted, the best degradation was achieved on acid pH (86.68%), which is followed by near neutral pH (63.7%) and basic pH (57.1%). Chaudhari et al. [55] reported a maximum of 65% degradation of MTC with TiO_2 as a photocatalyst in 2 h of reaction and similar pH and solar irradiation conditions.

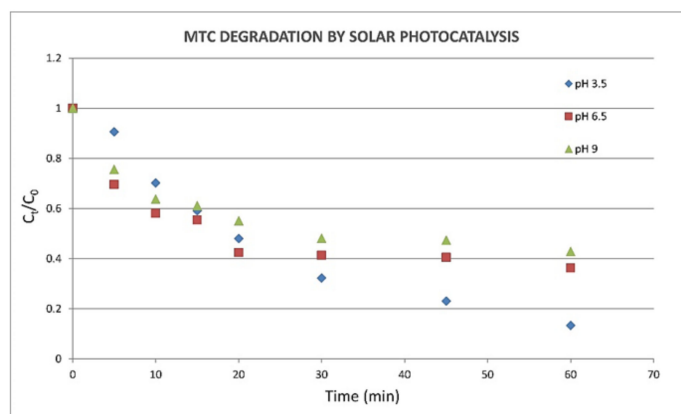


Figure 4. MTC degradation by solar heterogeneous photocatalysis at different pH (3.5, 6.5, and 9), without H_2O_2 addition.

In the other hand, in neutral pH conditions, the best degradation (69.44%) was obtained when 0.5 mM of H_2O_2 was added, but as can be seen, this result is lower than found in acid pH. Meanwhile, when MTC was treated in basic pH conditions, a degradation of 18.74% was obtained with 1 mM H_2O_2 addition, 38.43% when 0.5 mM was added, and 57.17% without dosage of oxidant agent (Table 1).

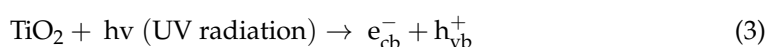
In 2015, Benhabiles et al. [54] reported a 98% degradation of MTC after 120 min of reaction in pH 11, but, as can be seen, our results yield a different conclusion: the lowest results for MTC degradation were obtained in basic pH. In agreement with what was reported by Zaruma et al. [51], it was possible to observe that in higher pH, there exists a saturation and coloration of the catalyst impregnated in the glass plate, which the authors believe is an explanation for low degradation results under basic pH.

2.3. Kinetic Analysis Results

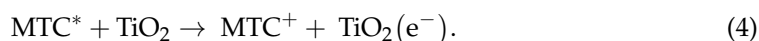
The kinetic constants (K_{ph} and K_{phC}) and half lifetime ($\tau_{1/2}$) were calculated for experiments performed with the addition of H_2O_2 and in the absence of this oxidant agent. Kinetic data are presented in Table 1, considering first-order reaction for photolysis and photocatalysis experiments after 60 min of experimentation, under the three pH values tested.

The hindering of degradation reactions could be caused by an H_2O_2 addition in a too high dose. According to Wang and Xu [56], H_2O_2 addition increases degradation up to a certain point, but when the peroxide presence is too high, it inhibits the photolytic degradation of organic compounds.

It is well known that MTC is photosensitized under visible light illumination, in a process where the molecule is excited instead of the photocatalyst, as shown in Equation (2) [56]. In photolysis experiments, the degradation depends upon photosensitization of the MTC, while in photocatalysis, a combination of both processes takes place: radiation excites both molecules, the UV portion of solar radiation excites TiO_2 , while the visible portion excites the MTC directly, so the total spectrum of solar radiation is used, as shown in Equation (3).



Excited MTC can also react with TiO_2 in photocatalytic processes, as shown in Equation (4):



Given this, better degradation was expected on photocatalysis experiments, as both pathways for MTC degradation are taking place, and more of the solar radiation spectrum is useful for degradation.

Zaruma et al. [51] reported in their study that using a UV-C lamp as a radiation source and under pH of 3.5, better results were reached in absence in the photocatalyst, and they explained their results as a product of the H_2O_2 /UV-C interaction, given that H_2O_2 , when irradiated with UV-C radiation, yields OH radicals [57]. As this study reports results from solar processes, no UV-C radiation reached H_2O_2 molecules, discarding this pathway for degradation and thus explaining that H_2O_2 addition did not improve results.

In the past, electrostatic interactions between photocatalyst and pollutant have been reported to play a role in photocatalysis experiments [58]; as MTC is a cationic molecule [49,59], better results from photocatalysis experiments were expected from basic pH when TiO_2 is negatively charged [60–62]. Instead, such electrostatic attraction appears to be detrimental for degradation, given a possible color saturation by the photocatalyst as, according to Houas et al. [49], the adsorption of MTC on TiO_2 increases as pH increases. However, again, in control photocatalysis experiments, MTC degradation was never higher than 10%, so the adsorption of MTC on the photocatalyst was discarded as the mechanism behind degradation shown in Table 1.

2.4. Statistical Analysis Results

Student's *t*-test, which was used to compare the reaction rate constants from both photolysis and photocatalysis experiments, showed that in almost all the cases of pH conditions and H_2O_2 addition, rates are different from each other ($p < 0.05$), but not the ones obtained under pH 9 and with 0.5 mM/L of the oxidant agent addition. These results

coincide with the percentages of degradation reported in Table 1; in these conditions, the degradation percentages reached for photolysis and photocatalysis are very close (36.53% and 38.43%, respectively). Student-t analysis allowed authors to assure that both processes, when compared under the same conditions, throw statistically different results.

ANCOVA analysis, where MTC degradation was the response variable, showed significant differences ($p < 0.05$) for all the samples regarding the process (photolysis and photocatalysis) and pH level (acidic, neutral, and basic) (Figure 5). For the H_2O_2 factor (0, 0.5, and 1 mM/L), significant differences were found in times of 10, 20, 30, and 60 min.

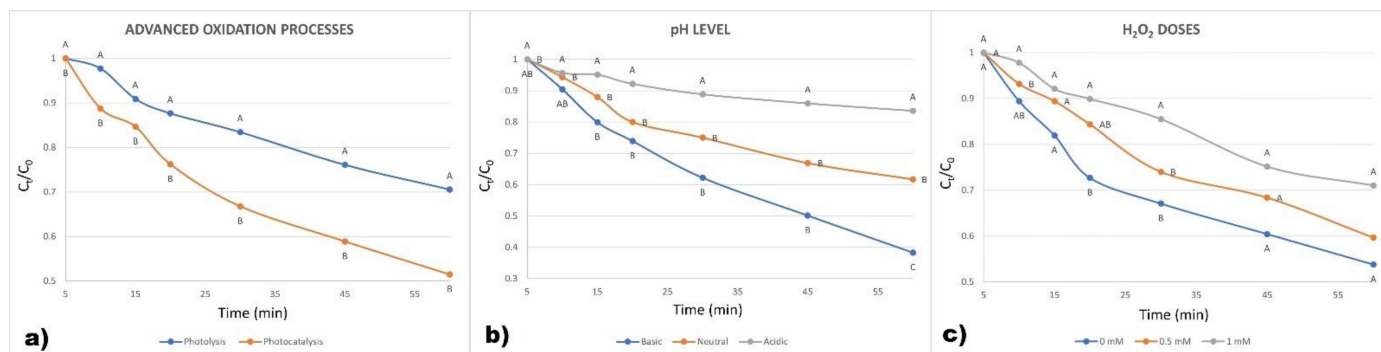


Figure 5. Comparison of MTC concentration means in every sampling time for (a) photolysis and photocatalysis processes, (b) initial pH: 3.5, 6.5, and 9, and (c) H_2O_2 dose. The different capital letters (A, B, C) within the figure indicate statistically significant differences ($p < 0.05$) in the mean MTC concentration value for every sampling time (horizontal axis).

In the experiments, MTC degradation was found to be dependent of the applied process, H_2O_2 presence, and pH of the solution.

2.5. Collector Area per Order (A_{CO}) Estimation

A comparative estimation of the A_{CO} , (m^2/m^3 -order) for MTC degradation by photolysis and heterogeneous photocatalysis processes is shown in Table 2, utilizing the method for solar energy-driven systems based on a first-order reaction ($n = 1$), taking place in a batch reactor and a low concentration [63]. Table 2 shows the effect of the H_2O_2 dose or not on A_{CO} estimation for both photolysis and heterogeneous photocatalysis processes at pH 3.5, under the same experimental conditions and at noon, following Equation (9).

Table 2. Estimation of A_{CO} , (m^2/m^3 -order) and comparative efficiency for both photolytic and heterogeneous photocatalytic processes, $\epsilon = [(A_{CO_{\text{photol}}} - A_{CO_{\text{photocat}}}) / (A_{CO_{\text{photol}}})] \times 100$, for MTC degradation, based on a first-order reaction ($n = 1$), taking place in a batch reactor and a low concentration (30 mg/L), in acidic conditions (pH 3.5), in experiments at noon.

H_2O_2 (mM/L)	Photolysis	Photocatalysis	Efficiency (ϵ)
	A_{CO} (m^2/m^3 -Order)	A_{CO} (m^2/m^3 -Order)	
0	97	56	42.26%
0.5	137	81	40.87%
1	136	78	42.64%

Bandala and Estrada [64] reported similar A_{CO} magnitudes to the ones here presented for comparison of four different solar collection geometries. In all cases, for application to the photocatalytic degradation of oxalic acid, the collection area was $0.75 m^2$, where TiO_2 was employed as the catalyst by homogeneous photocatalysis, and the solution was recirculated at 168 L/: parabolic trough concentrator (PTC), $A_{CO} = 25 m^2/m^3$ -order; V trough collector (VTC), $A_{CO} = 38 m^2/m^3$ -order; compound parabolic concentrator

(CPC), $A_{CO} = 34 \text{ m}^2/\text{m}^3$ -order, when TiO_2 concentration is 0.01 g/L, and flat tubular (FT), $A_{CO} = 35 \text{ m}^2/\text{m}^3$ -order, when TiO_2 is 0.05 g/L.

The lower the collector area per order, the higher the efficiency of the process. In this regard, A_{CO} estimation (m^2/m^3 -order) shows better magnitude for MTC solar heterogeneous photocatalytic degradation than that from photolysis (Table 2), so the photocatalysis efficiency is always higher ($\epsilon > 40\%$) in all experiments performed in pH of 3.5, with and without H_2O_2 addition. The best $A_{CO} = 56 \text{ m}^2/\text{m}^3$ -order was obtained for photocatalysis without H_2O_2 (Table 2). These results are in agreement with the MTC kinetic degradation reported in Table 1, confirming the better efficiency for the photocatalysis process to the one from photolysis.

3. Materials and Methods

3.1. Flat Plate Solar Reactor

A SPR (Figure 6) with a metal base and an acrylic plastic container was used, which supports a flat glass plate with a contact area of 0.1 m^2 ($0.3 \text{ m} \times 0.33 \text{ m}$) and has a slope of 20° with respect to the horizontal. The SPR was adjusted to Durango City, México latitude ($24^\circ 1' 40'' \text{ N}$), so it can receive the greatest amount of sunlight [65]. The reactor maintains a constant flow (127 L/h) in the laminar regime ($\text{Re} < 1000$), recirculating the solution from a collection tank [66].

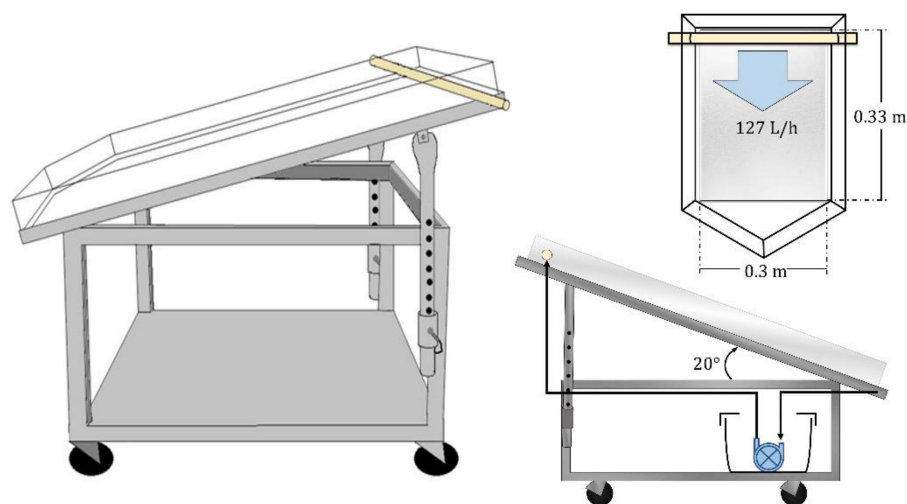


Figure 6. Flat plate solar reactor in batch mode with 0.1 m^2 contact area set at a 20° of inclination and constant flow of 127 L/h in order to achieve a laminar flow regime ($\text{Re} < 1000$).

3.2. Process and Experimental Design for the Study

Experiments were carried out for the degradation of MTC (HYCEL, Zapopan, Jal., Mexico) in aqueous solution by photolysis and photocatalysis with TiO_2 (Fermont, Monterrey, N.L., Mexico) as the photocatalyst, which was impregnated by direct spraying on the glass plate, using the method proposed by Stintzing [67].

In relation to the initial concentration of MTC to be degraded, the work of Stintzing was taken into account [67], where a concentration of $25 \text{ g}/\text{m}^2$ de TiO_2 was optimal for the degradation of MTC at an initial concentration of 250 mg/L, which is a relationship similar to that used in this work where the concentration of the photocatalyst was $2 \text{ g}/\text{m}^2$ in order to degrade 30 mg/L of MTC. The previous concentration ($2 \text{ g}/\text{m}^2$) has shown to be the optimal photocatalyst mass-support surface ratio used by this research group, since it presented the best results for the degradation of organic pollutants such as 2,5-dichlorophenol [31,41,68], and cytostatic contaminants such as 6-mercaptopurine [37]. It has also proven its effectiveness for the inactivation of fecal coliforms [58].

Table 3 shows the proportions of TiO_2 photocatalyst on different supports (g/m^2) for the degradation of MTC and other dyes. Alinsafi et al. [69] and Zahraa et al. [70]

used a concentration of photocatalyst (TiO₂) slightly higher than that used in this work, with 2.8 g/m², while Maleki and Bertola [71] used a considerably lower proportion with 0.35 g/m².

Table 3. Degradation of MTC and other dyes by heterogeneous photocatalysis with different concentrations of TiO₂ on various supports.

Support	Catalyst	TiO ₂ (g/m ²)	Dye Initial Concentration	Radiation	Degradation (%)	Ref.
Concrete	TiO ₂ -P25	25	³ MTC	Solar radiation	80	[67]
Glass slides	TiO ₂ -P25	2.8	⁴ BDR (50 mg/L)	UV lamp	94	[69]
			⁵ YCDG (50 mg/L)		89	
Glass plate	TiO ₂	2.8	⁶ DY (25 mg/L)	UV lamp	~60	[70]
			DY (25 mg/L)	Solar radiation	~45	
			⁷ DB (25 mg/L)	UV lamp	~80	
¹ PP	TiO ₂ -P25	0.35	MTC (4 mg/L)	UV lamp	~90	[71]
Glass plate	Titanium (IV) oxide (99% anatase)	6.5	MTC (20 mg/L)	UV-vis lamp	96.1	[72]
		39			98.68	
² ACF	TiO ₂ /ACF	4	MTC (40 mg/L)	UV lamp	99	[73]
Glass plate	P25-TiO ₂ /ENR/PVC composites	15	MTC (12 mg/L)	UV lamp	99.49	[74]

¹ polpropylene, ² activated carbon fiber, ³ methylene blue, ⁴ black DR, ⁵ yellow CDG, ⁶ drimarene yellow, ⁷ drimarene black.

Two processes were considered for the experimental design: photolysis and photocatalysis; three pH levels: 3.5, 6.5, and 9; in the same way, three doses of H₂O₂ (0, 0.5, and 1 mM/L) were tested to verify the effect of the addition of oxidizing agent.

Each experiment lasted 60 min, with a volume of 2 L of sample and concentration of 30 mg/L of MTC, using distilled water for the preparation of the solutions. The experiments were performed under three pH magnitudes (3.5, 6.5, and 9) to check the pH effect on the contaminant degradation, and the initial pH was adjusted adding NaOH or HNO₃ solutions.

Similarly, the effect of an oxidizing agent was analyzed by adding different doses of hydrogen peroxide: no dose, 0.5, and 1 mM H₂O₂/L, which were added to the solution after pH adjustment. For the experiments without H₂O₂ dose, the experimental time began when the solution covered the whole glass plate contact area; for the experiments with H₂O₂ dose, the time began after the solution reached the whole contact area of the plate and the H₂O₂ was added.

Samples were taken at times of 5, 10, 15, 20, 30, 45, and 60 min. MTC degradation was followed by UV-Vis spectrophotometry at a wavelength of 670 nm for each experiment [75]. To ensure that H₂O₂ addition is not the only MTC degradation contributing factor, a series of control experiments were performed in the absence of radiation (under shadow) at different pH values.

Radiation, humidity, and temperature data were measured by the meteorological station of the Secretaría de Recursos Naturales y Medio Ambiente, which was measured by a WE300 Solar Radiation Sensor pyranometer (Global Water, Yellow Springs, OH, USA). Experiments were conducted on days with an absence of air currents, in an established

time range 12:00–13:00 h, in cloudless days of April–May months, with an average solar radiation incidence 980 W/m^2 , as shown in Figure 7.

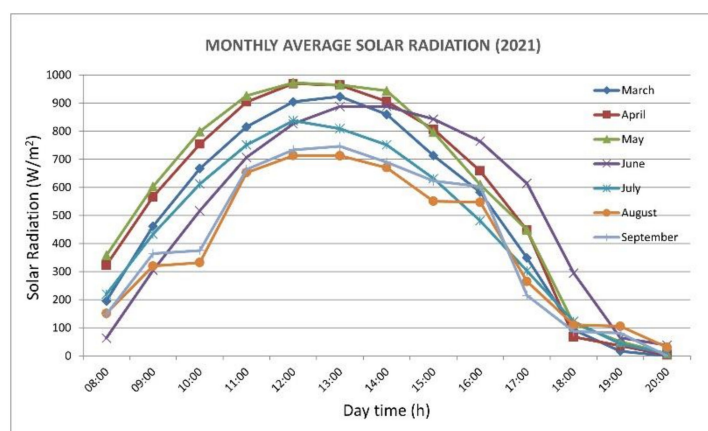


Figure 7. Average solar radiation between the months of March and September in the city of Durango.

A $2 \times 3 \times 3$ factorial design with covariates and repeated measures was used to analyze the degradation results and is described through Equation (5):

$$Y_{ijklm} = \mu + P_i + D_j + \text{pH}_k + t_1 + (a * t_1) + (b * t_2) + (c * r) + (d * H) + C_0 + (P * M)_{ij} + (P * \text{pH})_{ik} + (P * t)_{il} + (M * \text{pH})_{jk} + (M * t)_{jl} + (\text{pH} * t)_{kl} + \varepsilon_{ijklm}. \quad (5)$$

In Equation (5), the response variable corresponds to Y_{ijklm} , the general average of the model is μ , P_i is the process (photolysis $P_i = 1$ and photocatalysis $P_i = 2$), D_j is the H_2O_2 dose (no dose $D_j = 1$, 0.5 mM $D_j = 2$, and 1 mM $D_j = 3$), pH_k is the pH level (3.5, 6.5, and 9), C_0 is the initial concentration, r is the intensity of solar radiation, t_1 and t_2 correspond to the initial and final temperature, H is for humidity, and ε_{ijklm} represents the error.

3.3. Kinetic Analysis

The experimental data kinetic analysis was performed considering a first-order reaction ($n = 1$) [46]. Equation (6) was utilized to calculate the degradation rate constant of the experiments [46,51]. More information about Equation (6) can be found in Supplementary Materials (Section S2).

$$(X)_t = (X)_0 e^{-(K_{\text{phC}}) \cdot t}. \quad (6)$$

In Equation (6), X_t is the concentration of MTC over time, X_0 represents the MTC solution initial concentration, and K_{phC} corresponds to photocatalytic rate constant.

The photolytic constant (K_{ph}) was determined by formal kinetics [76], and the half-life time calculation ($\tau_{1/2}$) was obtained by Equation (7) [44]

$$\tau_{1/2} = \frac{\ln(2)}{k}. \quad (7)$$

3.4. Statistical Analysis

Student's t -test (Equation (8)) was used in order to compare the MTC degradation kinetic constants from photolysis and photocatalysis processes performed under the same initial pH and H_2O_2 addition. An analysis of covariance (ANCOVA) allowed authors to evaluate the effect of the factors considered by the experimental design, using an $\alpha = 0.05$.

ANCOVA was performed using the SAS Studio 9.0 (SAS Institute Inc., Cary, NC, USA) statistical package, and the Gauss–Markov assumptions were verified.

$$t = \frac{k_1 - k_2}{\sqrt{\frac{\sigma_1^2}{n_1} + \frac{\sigma_2^2}{n_2}}} \quad (8)$$

In Equation (8), t represents the Student's t statistics, k_1 and k_2 represent the photocatalytic (K_{phC}) and photolytic (K_{ph}) reaction constants, respectively; variances are represented by σ_1^2 and σ_2^2 , and the number of observations is represented by n_1 and n_2 .

3.5. Solar Energy-Driven System

In this study, MTC pollutant degradation was carried out in a solar flat plate reactor; consequently, the standard figures of merit suggested by IUPAC [63] can be utilized for the evaluation of AOPs in the aspects of energy requirements or area required.

The collector area per order (A_{CO}) (m^2/m^3 -per order) is the collector area required to reduce the concentration in polluted water by one order of magnitude in a time t , in a unit volume (e.g., $1 m^3$), when the incident solar irradiance is $1000 W/m^2$ [63]. A_{CO} was calculated by Equation (9), using the method for solar energy-driven systems based on a first-order reaction ($n = 1$), taking place in a batch reactor and a low concentration [63]:

$$A_{CO} = \frac{A \cdot \bar{E}_S \cdot t}{V \cdot \log\left(\frac{c_i}{c_f}\right)} \quad (9)$$

In Equation (9), A_{CO} is the collector area per order (m^2/m^3 -order), A is the reaction area of the reactor, \bar{E}_S is the average solar irradiance over the time of a given treatment, t is the treatment time, V is the unit volume treated of pollutant, and c_i and c_f are the influent and effluent pollutant concentrations.

4. Conclusions

In the absence of solar radiation, the experiments performed did not show remarkable MTC degradation, not even when H_2O_2 was added as an oxidant agent at the beginning of the experiment.

H_2O_2 addition in control experiments does not show degradation, but in experiments in the presence of radiation, it actually hinders the degradation; the authors believe that this is an indication of competence for radiation between MTC and peroxide molecules.

The experiments performed in the presence of a photocatalyst were always better than those of photolysis. The highest degradation (86.68%) was reached in a photocatalysis experiment without H_2O_2 addition and in acidic pH 3.5.

In photolysis experiments, the degradation depends upon photosensitization of the MTC, while in photocatalysis, a combination of both processes takes place: radiation excites both molecules, the UV portion of solar radiation excites TiO_2 , while the visible portion excites the MTC directly. Better degradation was expected on photocatalysis experiments, as both pathways for MTC degradation are taking place, and more of the solar radiation spectrum is useful for degradation.

The ANCOVA results for MTC degradation fulfilled the Gauss–Markov assumptions and showed significant differences ($p < 0.05$) for all the times with respect to the process (photolysis and photocatalysis) and pH level (acidic, neutral, and basic).

A_{CO} estimation (m^2/m^3 -order) shows better magnitude for MTC solar heterogeneous photocatalytic degradation than that from photolysis, so photocatalysis efficiency is always higher ($\epsilon > 40\%$) in all experiments performed at a pH of 3.5, with and without H_2O_2 addition.

Supplementary Materials: The following supporting information can be downloaded at: <https://www.mdpi.com/article/10.3390/catal12020132/s1>, S1: General mechanism for reactive radical species by photocatalysis and S2: Photocatalytic rate constant (K_{pHC}) calculations.

Author Contributions: Data curation, P.E.Z.-A.; formal analysis, P.E.Z.-A., L.A.G.-B. and J.B.P.-N.; funding acquisition, J.B.P.-N.; investigation, P.E.Z.-A., L.A.G.-B., C.M.N.-N. and J.B.P.-N.; methodology, C.M.N.-N., L.A.G.-B. and J.B.P.-N.; project administration, J.B.P.-N.; supervision, J.B.P.-N.; writing—original draft, P.E.Z.-A.; writing—review and editing, L.A.G.-B., C.M.N.-N. and J.B.P.-N. All authors have read and agree to the published version of the manuscript.

Funding: The first author wishes to extend his sincere appreciation to the Consejo Nacional de Ciencia y Tecnología (CONACyT) through the doctorate scholarship granted to first author, student identification B180614. Support was received also from Instituto Politécnico Nacional (IPN/SIP project 20210507) for funding this project. The content does not necessarily reflect the views and policies of the funding organizations.

Institutional Review Board Statement: Not applicable.

Informed Consent Statement: Not applicable.

Data Availability Statement: Data are contained within the article or Supplementary Materials.

Acknowledgments: The authors would also like to acknowledge the Planta de Tratamiento de Aguas Residuales Oriente for providing additional facilities to conduct the research, Centro de Investigación de Materiales Avanzados (CIMAV-Durango) for sample analysis and for access to its experimental facility.

Conflicts of Interest: The authors declare no conflict of interest.

References

1. Ruiz-Hitzky, E. Molecular access to intracrystalline tunnels of sepiolite. *J. Mater. Chem.* **2001**, *11*, 86–91. [[CrossRef](#)]
2. Santamarina, J.C.; Klein, K.A.; Wang, Y.H.; Prencke, E. Specific surface: Determination and relevance. *Can. Geotech. J.* **2002**, *39*, 233–241. [[CrossRef](#)]
3. Wang, R.; Guo, M.; Hu, Y.; Zhou, J.; Wu, R.; Yang, X. A Molecularly Imprinted Fluorescence Sensor Based on the ZnO Quantum Dot Core–Shell Structure for High Selectivity and Photolysis Function of Methylene Blue. *ACS Omega* **2020**, *5*, 20664–20673. [[CrossRef](#)] [[PubMed](#)]
4. Schirmer, R.H.; Adler, H.; Pickhardt, M.; Mandelkow, E. Lest we forget you-methylene blue. *Neurobiol. Aging* **2011**, *32*, 2325.e7–2325.e16. [[CrossRef](#)]
5. Jing, H.P.; Wang, C.C.; Zhang, Y.W.; Wang, P.; Li, R. Photocatalytic degradation of methylene blue in ZIF-8. *RSC Adv.* **2014**, *4*, 54454–54462. [[CrossRef](#)]
6. Harrison, B.J.; Triponez, F. Intraoperative adjuncts in surgery for primary hyperparathyroidism. *Langenbeck's Arch. Surg.* **2009**, *394*, 799–809. [[CrossRef](#)]
7. Pollack, G.; Pollack, A.; Delfiner, J.; Fernández, J. Parathyroid surgery and methylene blue: A review with guidelines for safe intraoperative use. *Laryngoscope* **2009**, *119*, 1941–1946. [[CrossRef](#)]
8. Van der Vorst, J.; Schaafsma, B.; Verbeek, F.; Swijnenburg, R.; Tummers, Q.; Hutteman, M.; Hamming, J.F.; Kievit, J.; Frangioni, J.; Van de Velde, C.; et al. Intraoperative near-infrared fluorescence imaging of parathyroid adenomas with use of low-dose methylene blue. *Head Neck* **2013**, *36*, 853–858. [[CrossRef](#)]
9. Borghei, Y.S.; Hosseini, M.; Ganjali, M.R. Visual detection of miRNA using peroxidase-like catalytic activity of DNA-CuNCs and methylene blue as indicator. *Clin. Chim. Acta* **2018**, *483*, 119–125. [[CrossRef](#)]
10. Rafiee-Pour, H.A.; Behpour, M.; Keshavarz, M. A novel label-free electrochemical miRNA biosensor using methylene blue as redox indicator: Application to breast cancer biomarker miRNA-21. *Biosens. Bioelectron.* **2016**, *77*, 202–207. [[CrossRef](#)]
11. Dos Santos, A.F.; Terra, L.F.; Wailemann, R.A.M.; Oliveira, T.C.; Gomes, V.M.; Mineiro, M.F.; Meotti, F.C.; Bruni-Cardoso, A.; Baptista, M.S.; Labriola, L. Methylene blue photodynamic therapy induces selective and massive cell death in human breast cancer cells. *BMC Cancer* **2017**, *17*, 194. [[CrossRef](#)]
12. Hosseinzadeh, R.; Khorsandi, K.; Jahanshahi, M. Combination photodynamic therapy of human breast cancer using salicylic acid and methylene blue. *Spectrochim. Acta-A Mol. Biomol. Spectrosc.* **2017**, *184*, 198–203. [[CrossRef](#)]
13. Da Collina, G.A.; Freire, F.; Santos, T.P.D.C.; Sobrinho, N.G.; Aquino, S.; Prates, R.A.; da Silva, D.D.F.T.; Tempestini-Horllana, A.C.R.; Pavani, C. Controlling Methylene Blue aggregation: A more efficient alternative to treat *Candida albicans* infections using Photodynamic Therapy. *Photochem. Photobiol. Sci.* **2018**, *17*, 1355–1364. [[CrossRef](#)]
14. Huang, Y.Y.; Wintner, A.; Seed, P.C.; Brauns, T.; Gelfand, J.A.; Hamblin, M.R. Antimicrobial photodynamic therapy mediated by methylene blue and potassium iodide to treat urinary tract infection in a female rat model. *Sci. Rep.* **2018**, *8*, 7257. [[CrossRef](#)]

15. Fito, J.; Abrham, S.; Angassa, K. Adsorption of Methylene Blue from Textile Industrial Wastewater onto Activated Carbon of *Parthenium hysterophorus*. *Int. J. Environ. Res.* **2020**, *14*, 501–511. [[CrossRef](#)]
16. Duran-Jimenez, G.; Hernandez-Montoya, V.; Montes-Moran, M.A.; Bonilla-Petriciolet, A.; Rangel-Vazquez, N.A. Adsorption of dyes with different molecular properties on activated carbons prepared from lignocellulosic wastes by Taguchi method. *Microporous Mesoporous Mater.* **2014**, *199*, 99–107. [[CrossRef](#)]
17. Dariani, R.S.; Esmaili, A.; Mortezaali, A.; Dehghanpour, S. Photocatalytic reaction and degradation of methylene blue on TiO₂ nano-sized particles. *Optik* **2016**, *127*, 7143–7154. [[CrossRef](#)]
18. Jawad, A.H.; Abdulhameed, A.S.; Mastuli, M.S. Acid-fractionalized biomass material for methylene blue dye removal: A comprehensive adsorption and mechanism study. *J. Taibah Univ. Sci.* **2020**, *14*, 305–313. [[CrossRef](#)]
19. Lv, X.-M.; Yang, X.-L.; Xie, X.-Y.; Yang, Z.-Y.; Hu, K.; Wu, Y.-J.; Jiang, Y.-Y.; Liu, T.-F.; Fang, W.-H.; Huang, X.-Y. Comparative transcriptome analysis of *Anguilla japonica* livers following exposure to methylene blue. *Aquac. Res.* **2017**, *49*, 1232–1241. [[CrossRef](#)]
20. Xu, T.; Wang, X.; Huang, Y.; Lai, K.; Fan, Y. Rapid detection of trace methylene blue and malachite green in four fish tissues by ultra-sensitive surface-enhanced Raman spectroscopy coated with gold nanorods. *Food Control* **2019**, *106*, 106720. [[CrossRef](#)]
21. Salh, D.M.; Aziz, B.K.; Kaufhold, S. High Adsorption Efficiency of Topkhana Natural Clay for Methylene Blue from Medical Laboratory Wastewater: A Linear and Nonlinear Regression. *Silicon* **2020**, *12*, 87–99. [[CrossRef](#)]
22. Payra, S.; Challagulla, S.; Bobde, Y.; Chakraborty, C.; Ghosh, B.; Roy, S. Probing the Photo- and Electro-catalytic Degradation Mechanism of Methylene Blue Dye Over ZIF-derived ZnO. *J. Hazard. Mater.* **2019**, *373*, 377–388. [[CrossRef](#)]
23. Guilloso, R.; Le Roux, J.; Mailler, R.; Vulliet, E.; Morlay, C.; Nauleau, F.; Gasperi, J.; Rocher, V. Organic micropollutants in a large wastewater treatment plant: What are the benefits of an advanced treatment by activated carbon adsorption in comparison to conventional treatment? *Chemosphere* **2019**, *218*, 1050–1060. [[CrossRef](#)]
24. Kishor, R.; Purchase, D.; Ferreira, L.F.R.; Mulla, S.I.; Bilal, M.; Bharagava, R.N. Environmental and Health Hazards of Textile Industry Wastewater Pollutants and Its Treatment Approaches. In *The Handbook of Environmental Chemistry*; Springer Nature: Basingstoke, UK, 2020; pp. 1–24. [[CrossRef](#)]
25. Kishor, R.; Purchase, D.; Saratale, G.D.; Saratale, R.G.; Ferreira, L.F.R.; Bilal, M.; Chandra, R.; Bharagava, R.N. Ecotoxicological and health concerns of persistent coloring pollutants of textile industry wastewater and treatment approaches for environmental safety. *J. Environ. Chem. Eng.* **2021**, *9*, 105012. [[CrossRef](#)]
26. Sharma, P.; Kaur, R.; Baskar, C.; Chung, W.J. Removal of methylene blue from aqueous waste using rice husk and rice husk ash. *Desalination* **2010**, *259*, 249–257. [[CrossRef](#)]
27. Gines-Palestino, R.S.; Oropeza-De la Rosa, E.; Montalvo-Romero, C.; Cantú-Lozano, D. Rheokinetic and effectiveness during the phenol removal in mescal vinasses with a rotary disks photocatalytic reactor (RDPR). *Rev. Mex. Ing. Quim.* **2020**, *19*, 639–652. [[CrossRef](#)]
28. Pavan, F.; Lima, E.; Dias, S.; Mazzocato, A. Methylene blue biosorption from aqueous solutions by yellow passion fruit waste. *J. Hazard. Mater.* **2008**, *15*, 703–712. [[CrossRef](#)]
29. Thakur, S.; Pandey, S.; Arotiba, O.A. Development of a sodium alginate-based organic/inorganic superabsorbent composite hydrogel for adsorption of methylene blue. *Carbohydr. Polym.* **2016**, *153*, 34–46. [[CrossRef](#)]
30. Adelin, M.A.; Gunawan, G.; Nur, M.; Haris, A.; Widodo, D.S.; Suyati, L. Ozonation of methylene blue and its fate study using LC-MS/MS. *J. Phys. Conf. Ser.* **2020**, *1524*, 012079. [[CrossRef](#)]
31. Morones-Esquivel, M.M.; Núñez-Núñez, C.M.; González-Burciaga, L.A.; Hernández-Mendoza, J.L.; Osorio-Revilla, G.I.; Proal-Nájera, J.B. Kinetics and statistical approach for 2,5-dichlorophenol degradation in short reaction time by solar TiO₂/glass photocatalysis. *Rev. Mex. Ing. Quim.* **2020**, *19*, 555–568. [[CrossRef](#)]
32. Núñez-Núñez, C.M.; Osorio-Revilla, G.I.; Villanueva-Fierro, I.; Antileo, C.; Proal-Nájera, J.B. Solar fecal coliform disinfection in a wastewater treatment plant by oxidation processes: Kinetic analysis as a function of solar radiation. *Water* **2020**, *12*, 639. [[CrossRef](#)]
33. López-Ojeda, G.; Vargas-Zavala, A.; Gutiérrez-Lara, M.; Ramírez-Zamora, R.; Duran-Moreno, A. Oxidación Foelectrocatalítica de fenol y 4-clorofenol con un soporte de titanio impregnado con TiO₂. *Rev. Int. Contam. Ambient.* **2011**, *27*, 75–84.
34. González-Burciaga, L.A.; Núñez-Núñez, C.M.; Proal-Nájera, J.B. Challenges of TiO₂ heterogeneous photocatalysis on cytostatic compounds degradation: State of the art. *Environ. Sci. Pollut. Res.* **2021**, 1–24. Available online: <https://link.springer.com/article/10.1007/s11356-021-17241-8> (accessed on 21 December 2021). [[CrossRef](#)] [[PubMed](#)]
35. Asghar, A.; Raman, A.A.A.; Daud, W.M.A.W. Advanced oxidation processes for in-situ production of hydrogen peroxide/hydroxyl radical for textile wastewater treatment: A review. *J. Clean. Prod.* **2015**, *87*, 826–838. [[CrossRef](#)]
36. Wang, J.; Wang, S. Reactive species in advanced oxidation processes: Formation, identification and reaction mechanism. *Chem. Eng. J.* **2020**, *401*, 126158. [[CrossRef](#)]
37. González-Burciaga, L.A.; Núñez-Núñez, C.M.; Morones-Esquivel, M.M.; Ávila-Santos, M.; Lemus-Santana, A.; Proal-Nájera, J.B. Characterization and comparative performance of TiO₂ photocatalysts on 6-mercaptopurine degradation by solar heterogeneous photocatalysis. *Catalysts* **2020**, *10*, 118. [[CrossRef](#)]
38. Sirés, I.; Brillas, E.; Oturan, M.A.; Rodrigo, M.A.; Panizza, M. Electrochemical advanced oxidation processes: Today and tomorrow. A review. *Environ. Sci. Pollut. Res.* **2014**, *21*, 8336–8367. [[CrossRef](#)]

39. Waghmode, T.R.; Kurade, M.B.; Sapkal, R.T.; Bhosale, C.H.; Jeon, B.H.; Govindwar, S.P. Sequential photocatalysis and biological treatment for the enhanced degradation of the persistent azo dye methyl red. *J. Hazard. Mater.* **2019**, *371*, 115–122. [[CrossRef](#)]
40. Pantoja-Espinoza, J.C.; Proal-Nájera, J.B.; García-Roig, M.; Cháirez-Hernández, I.; Osorio-Revilla, G. Eficiencias comparativas de inactivación de bacterias coliformes en efluentes municipales por fotólisis (UV) y por fotocatalisis (UV/TiO₂/SiO₂) Caso: Depuradora de Aguas de Salamanca, España. *Rev. Mex. Ing. Quim.* **2015**, *14*, 119–135.
41. Morones-Esquivel, M.M.; Pantoja-Espinoza, J.C.; Proal-Nájera, J.B.; Cháirez-Hernández, I.; Gurrola-Reyes, J.N.; Ávila-Santos, M. Uso de un reactor de placa plana (TiO₂/vidrio) para la degradación de 2,5-diclorofenol por fotocatalisis solar. *Rev. Int. Contam. Ambient.* **2017**, *33*, 605–616. [[CrossRef](#)]
42. Dean, J.C.; Oblinsky, D.J.; Rafiq, S.; Scholes, G.D. Methylene Blue Exciton States Steer Nonradiative Relaxation: Ultrafast Spectroscopy of Methylene Blue Dimer. *J. Phys. Chem. B* **2016**, *120*, 440–454. [[CrossRef](#)]
43. Feitz, A.J.; Boyden, B.H.; Waite, T.D. Evaluation of two solar pilot scale fixed bed photocatalytic reactors. *Water Res.* **2000**, *34*, 3927–3932. [[CrossRef](#)]
44. Freudenhammer, H.; Bahnemann, D.; Bouselmi, L.; Geissen, S.U.; Ghrabi, A.; Saleh, F.; Si-Salah, A.; Siemon, V.; Vogelpohl, A. Detoxification and recycling of wastewater by solar-catalytic treatment. *Water Sci. Technol.* **1997**, *35*, 149–156. [[CrossRef](#)]
45. Malato, S.; Blanco, J.; Maldonado, M.I.; Fernández, P.; Alarcón, D.; Collares, M.; Farinha, J.; Correia de Oliveira, J. Engineering of solar photocatalytic collectors. *Sol. Energy* **2004**, *77*, 513–524. [[CrossRef](#)]
46. Malato, S.; Fernández-Ibáñez, P.; Maldonado, M.I.; Blanco, J.; Gernjak, W. Decontamination and disinfection of water by solar photocatalysis: Recent overview and trends. *Catal. Today* **2009**, *147*, 1–59. [[CrossRef](#)]
47. Braham, R.J.; Harris, A.T. Review of Major Design and Scale-up Considerations for Solar Photocatalytic Reactors. *Ind. Eng. Chem. Res.* **2009**, *48*, 8890–8905. [[CrossRef](#)]
48. Bergmann, K.; O’Konski, C.T. A spectroscopic study of methylene blue monomer, dimer, and complexes with montmorillonite. *J. Phys. Chem.* **1963**, *67*, 2169–2177. [[CrossRef](#)]
49. Houas, A.; Lachheb, H.; Ksibi, M.; Elaloui, E.; Guillard, C.; Herrmann, J. Photocatalytic degradation pathway of methylene blue in water. *Appl. Catal. B-Environ.* **2001**, *31*, 145–157. [[CrossRef](#)]
50. Chen, J.; Cesario, T.C.; Rentzepis, P.M. Effect of pH on Methylene Blue Transient States and Kinetics and Bacteria Photoinactivation. *J. Phys. Chem. A* **2011**, *115*, 2702–2707. [[CrossRef](#)]
51. Zaruma-Arias, P.E.; Núñez-Núñez, C.M.; Villanueva-Fierro, I.; Cháirez-Hernández, I.; Lares-Assef, I.A.; Gurrola-Reyes, J.N.; Proal-Nájera, J.B. Methylthionine chloride degradation on pilot UV-C reactors: Kinetics of photolytic and heterogeneous photocatalytic reactions. *Rev. Mex. Ing. Quim.* **2021**, *20*, 649–662. [[CrossRef](#)]
52. Zhou, Y.; Shuai, L.; Jiang, X.; Jiao, F.; Yu, J. Visible-light-driven photocatalytic properties of layered double hydroxide supported-Bi₂O₃ modified by Pd(II) for methylene blue. *Adv. Powder Technol.* **2015**, *26*, 439–447. [[CrossRef](#)]
53. Djellabi, R.; Ghorab, M.F.; Sehili, T. Simultaneous Removal of Methylene Blue and Hexavalent Chromium from Water Using TiO₂/Fe(III)/H₂O₂/Sunlight. *Clean-Soil Air Water* **2017**, *45*, 1500379. [[CrossRef](#)]
54. Benhabiles, O.; Mahmoudi, H.; Lounici, H.; Goosen, M.F.A. Effectiveness of a photocatalytic organic membrane for solar degradation of methylene blue pollutant. *Desalin. Water Treat.* **2015**, *57*, 14067–14076. [[CrossRef](#)]
55. Chaudhari, S.M.; Gawal, P.M.; Sane, P.K.; Sontakke, S.M.; Nemade, P.R. Solar light-assisted photocatalytic degradation of methylene blue with Mo/TiO₂: A comparison with Cr- and Ni-doped TiO₂. *Res. Chem. Intermed.* **2018**, *44*, 3115–3134. [[CrossRef](#)]
56. Wang, J.L.; Xu, L.J. Advanced Oxidation Processes for Wastewater Treatment: Formation of Hydroxyl Radical and Application. *Crit. Rev. Env. Sci. Technol.* **2012**, *42*, 251–325. [[CrossRef](#)]
57. Cubillas, A.M.; Schmidt, M.; Scharrer, M.; Euser, T.G.; Etzold, B.J.M.; Taccardi, N.; Wasserscheid, P.; Russell, P.S.J. Ultra-Low Concentration Monitoring of Catalytic Reactions in Photonic Crystal Fiber. *Chem. Eur. J.* **2012**, *18*, 1586–1590. [[CrossRef](#)]
58. Núñez-Núñez, C.M.; Cháirez-Hernández, I.; García-Roig, M.; García-Prieto, J.C.; Melgoza-Alemán, R.M.; Proal-Nájera, J.B. UV-C/H₂O₂ heterogeneous photocatalytic inactivation of coliforms in municipal wastewater in a TiO₂/SiO₂ fixed bed reactor: A kinetic and statistical approach. *React. Kinet. Mech. Catal.* **2018**, *125*, 1159–1177. [[CrossRef](#)]
59. Nuñez, S.C.; Yoshimura, T.M.; Ribeiro, M.S.; Junqueira, H.C.; Maciel, C.; Coutinho-Neto, M.D.; Baptista, M.S. Urea enhances the photodynamic efficiency of methylene blue. *J. Photochem. Photobiol. B Biol.* **2015**, *150*, 31–37. [[CrossRef](#)] [[PubMed](#)]
60. Calzada, L.A.; Castellanos, R.; García, L.A.; Klimova, T.E. TiO₂, SnO₂ and ZnO catalysts supported on mesoporous SBA-15 versus unsupported nanopowders in photocatalytic degradation of methylene blue. *Microporous Mesoporous Mater.* **2019**, *285*, 247–258. [[CrossRef](#)]
61. Schneider, O.M.; Liang, R.; Bragg, L.; Jaciw-Zurakowsky, I.; Fattahi, A.; Rathod, S.; Peng, P.; Servos, M.R.; Zhou, Y.N. Photocatalytic Degradation of Microcystins by TiO₂ Using UV-LED Controlled Periodic Illumination. *Catalysts* **2019**, *9*, 181. [[CrossRef](#)]
62. Harris, J.; Silk, R.; Smith, M.; Dong, Y.; Chen, W.T.; Waterhouse, G.I.N. Hierarchical TiO₂ Nanoflower Photocatalysts with Remarkable Activity for Aqueous Methylene Blue Photo-Oxidation. *ACS Omega* **2020**, *5*, 18919–18934. [[CrossRef](#)]
63. Bolton, J.R.; Bircher, K.G.; Tumas, W.; Tolman, C.A. Figures-of-merit for the technical development and application of advanced oxidation technologies for both electric- and solar-driven systems (IUPAC Technical Report). *Pure Appl. Chem.* **2009**, *73*, 627–637. [[CrossRef](#)]
64. Bandala, E.R.; Estrada, C. Comparison of solar collection geometries for application to photocatalytic degradation of organic contaminants. *J. Sol. Energy Eng.* **2007**, *129*, 22–26. [[CrossRef](#)]

65. Blanco, J. El reactor solar fotocatalítico: Estado del arte. In *Tecnologías Solares Para la Desinfección y Descontaminación de Agua (SOLARSAFEWATER)*; Blesa, M.A., Blanco, J., Eds.; ByToner: La Plata, Argentina, 2005; pp. 277–301.
66. Pantoja, J.C. Estudio de la Degradación de Materia Orgánica Presente en Aguas Residuales Municipales Mediante el Uso de Dióxido de Titanio (TiO₂) Como Fotocatalizador. Ph.D. Thesis, Centro Interdisciplinario de Investigación y Desarrollo Integral Regional Unidad Durango, Instituto Politécnico Nacional, Durango, México, 2015.
67. Stintzing, A. Solar Photocatalytic Treatment of Textile Wastewater at a Pilot Plant in Menzel Temime/Tunisia. Ph.D. Thesis, Institut für Thermische Verfahrenstechnik der Technischen Universität Clausthal, Clausthal, Germany, 2003.
68. Irigoyen-Campuzano, R.; González-Béjar, M.; Pino, E.; Proal-Nájera, J.B.; Pérez-Prieto, J. A Metal-Free, Nonconjugated Polymer for Solar Photocatalysis. *Chemistry* **2017**, *23*, 2867–2876. [[CrossRef](#)]
69. Alinsafi, A.; Evenou, F.; Abdulkarim, E.M.; Pons, M.N.; Zahraa, O.; Benhammou, A.; Yaacoubi, A.; Nejmeddine, A. Treatment of textile industry wastewater by supported photocatalysis. *Dyes Pigm.* **2007**, *74*, 439–445. [[CrossRef](#)]
70. Zahraa, O.; Maire, S.; Evenou, F.; Hachem, C.; Pons, M.N.; Alinsafi, A.; Bouchy, M. Treatment of wastewater dyeing agent by photocatalytic process in solar reactor. *Int. J. Photoenergy* **2006**, *2006*, 046961. [[CrossRef](#)]
71. Maleki, H.; Bertola, V. TiO₂ Nanofilms on Polymeric Substrates for the Photocatalytic Degradation of Methylene Blue. *ACS Appl. Nano Mater.* **2019**, *2*, 7237–7244. [[CrossRef](#)]
72. Jawad, A.H.; Alkarkhi, A.F.M.; Mubarak, N.S.A. Photocatalytic decolorization of methylene blue by an immobilized TiO₂ film under visible light irradiation: Optimization using response surface methodology (RSM). *Desalin. Water Treat.* **2014**, *56*, 161–172. [[CrossRef](#)]
73. Jain, P.; Kumar, A.; Verma, N.; Gupta, R.K. In-situ synthesis of TiO₂ nanoparticles in ACF: Photocatalytic degradation under continuous flow. *Sol. Energy* **2019**, *189*, 35–44. [[CrossRef](#)]
74. Nawari, M.A.; Zain, S.M. Enhancing the surface properties of the immobilized Degussa P-25 TiO₂ for the efficient photocatalytic removal of methylene blue from aqueous solution. *Appl. Surf. Sci.* **2012**, *258*, 6148–6157. [[CrossRef](#)]
75. Chaparro, C.V.; Cabanzo, R.; Mejía, E. Estudio de la adsorción de azul de metileno sobre dióxido de grafeno. *Rev. Colomb. Mater.* **2014**, *5*, 131–139.
76. Kuhn, H.; Försterling, H. Chemical kinetics. In *Principles of Physical Chemistry*, 2nd ed.; John Wiley & Sons, Ltd.: Chichester, UK, 2000; pp. 735–794.